Active earth thrust on walls supporting granular soils: effect of wall movement

Pression active des terres sur des murs soutenant des sols granulaires: l'effet du mouvement du mur

Loukidis D.
University of Cyprus, Cyprus

Salgado R.
Purdue University, USA

ABSTRACT: The methods currently used in the design practice of retaining walls supporting granular soils (sand, gravel, silt, and their mixtures) assume that the soil friction angle and, consequently, the active earth pressure coefficient K_A are independent of wall movement. However, the mobilized friction angle inside the retained soil in reality first reaches a peak value and then decreases towards to the critical state value as shear strain increases with wall movement. This study aims to investigate the development and evolution of the active earth pressure by modeling the soil mechanical behavior in a realistic way in a series of finite element analyses. Based on the numerical results, an equation is proposed for the estimation of K_A as a function of the initial relative density and the wall crest displacement.

RÉSUMÉ : Les méthodes actuellement utilisées dans la pratique de la conception des murs de soutènement supportant des sols granulaires (sable, gravier, limon et leurs mélanges) supposent que l'angle de frottement du sol et, par conséquent, le coefficient de pression active des terres K_A sont indépendantes du mouvement du mur. Toutefois, l'angle de frottement mobilisé à l'intérieur du sol retenu atteint en réalité d'abord une valeur de pic, puis diminue vers la valeur d'état critique à mesure que la déformation en cisaillement augmente avec le mouvement du mur. Cette étude vise à étudier le développement et l'évolution de la pression active des terres par la modélisation du comportement mécanique des sols de manière réaliste dans une série d'analyses par éléments finis. Sur la base des résultats numériques, une équation est proposée pour l'estimation de K_A en fonction de la densité relative initiale et le déplacement en crête du mur.

KEYWORDS: retaining wall, active earth pressure, sands, finite element analysis.

1 INTRODUCTION

The active earth pressure is expressed as the product of the vertical effective stress σ'_v in the retained soil mass or backfill and the active earth pressure coefficient K_A. The earliest and simplest methods for the calculation of the active earth pressure for purely frictional soils are those based on the Coulomb and Rankine theories. For a retained soil with horizontal free surface and a vertical wall backface, Coulomb's solution yields

$$K_A = \frac{\cos^2\phi}{\cos\delta\left[1+\sqrt{\dfrac{\sin(\phi+\delta)\sin\phi}{\cos\delta}}\right]^2} \tag{1}$$

The Coulomb solution can be proven to be equivalent to a rigorous limit analysis upper bound solution. It is also in good agreement with other upper bound solutions (Chen 1975, Soubra and Macuh 2002), as well as the lower bound solution by Lancellotta (2002), with the differences not exceeding 7%.

Furthermore, these methods, which are currently used in design practice, assume that ϕ and, consequently, the active earth pressure coefficient K_A are constant, i.e. their values do not change as the wall moves. However, the value of the mobilized friction angle in reality depends on a number of factors, such as the current mean effective stress, and, most importantly, the shear strain. Granular soils, unless in a very loose state, are strain-softening materials, meaning that the mobilized friction angle first reaches a peak value ϕ_p and then decreases towards to the critical state value ϕ_c. Hence, the active state developing inside the mass of the supported soil is a function of the wall movement.

The goal of this study is to investigate the development and evolution of the active earth pressure as the wall moves away from the retained soil using finite element (FE) analysis. The study focuses on retaining wall that are free to translate and rotate, such as gravity walls, cantilever walls and self-supported (cantilevered) sheet pile, secant pile or slurry walls. The mechanical behavior of the soil is captured realistically using a two-surface constitutive model based on critical state soil mechanics.

2 FINITE ELEMENT METHODOLOGY

The FE analyses were performed using the code SNAC (Abbo and Sloan 2000). A typical finite element mesh is shown in Fig. 1. The mesh consists of 8-noded, plane-strain quadrilateral elements and includes the wall, the supported soil and the foundation soil. The free surface of the supported soil is horizontal and without surcharge. The wall has a rectangular cross-section with width B and height H, and is modeled as a linear elastic material with very large Young's modulus so that it can be considered rigid. The retaining wall is also embedded a small distance D into the foundation soil. The analyses start with the supported soil at rest (K_0 state). No interface elements are placed between the soil and the wall. As a consequence, slippage between the wall and retained soil occurs due to the formation inside the soil mass of a shear band parallel to the wall backface. This roughness condition is realistic for walls made out of concrete; however, this may not be the case for sheet pile walls.

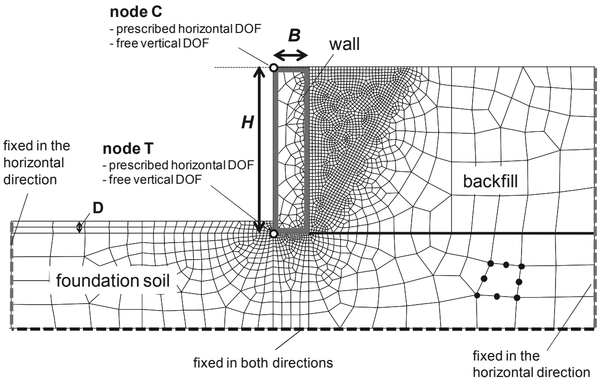

Figure 1. Typical mesh and boundary conditions used in the FE analyses.

The constitutive model used in this study is the two-surface plasticity model based on critical state soil mechanics developed originally by Manzari and Dafalias (1997) and subsequently modified by Dafalias et al. (2004) and Loukidis and Salgado (2009). The model parameters were determined by Loukidis and Salgado (2009) for two sands: air-pluviated/dry-deposited Toyoura sand and Ottawa sand. The model takes into account inherent and stress-induced anisotropy, and predicts accurately the soil response at both small and large strain regimes.

Because the problem under investigation involves material softening, the numerical simulations were inherently unstable. For this reason, the analyses were performed under displacement control. In the beginning of the analysis, the wall is fully supported at two points, namely the crest (node C) and the toe (node T), shown in Fig. 1, where the corresponding horizontal reactions are $R_{C,0}$ and $R_{T,0}$, respectively. Equivalently, the wall is initially prevented to move horizontally or rotate because of the external application of a horizontal force $F_{ext,0} = R_{C,0} + R_{T,0}$ and a moment $M_{ext,0} = R_{C,0}/H$. The analysis proceeds by the application of horizontal displacement increments Δu_C and Δu_T pointing away from the retained soil. As a result, the reactions F_{ext} ($=R_C + R_T$) and $M_{ext} = R_C/H$ begin to decrease. These displacement increments are applied in such way that the ratio $F_{ext}/F_{ext,0}$ is maintained equal to the ratio $M_{ext}/M_{ext,0}$. As a consequence, the prescribed displacements u_C and u_T are not equal to each other, leading to an overall wall motion that includes both translation and rotation. The wall is allowed to move vertically as no restraints are imposed on its nodes in the vertical direction.

3 SIMULATION RESULTS

Finite element analyses were performed for B ranging from 1.5m to 2.5m and H ranging from 6m to 8m. The sand unit weight γ was set equal to 18kN/m^3, while the coefficient K_0 was set equal to 0.5. For the sake of simplicity, the foundation soil is assumed to be of the same type and density as the retained soil.

3.1 *Failure mechanism*

Fig. 2 shows contours of the incremental maximum shear strain γ_{max} at the final stages of the simulations. The failure mechanism inside the supported soil consists of a wedge shaped sliding mass delimited by the wall backface and an oblique shear band originating from the heel of the wall. It can be seen also that families of secondary shear bands develop inside the sliding wedge. This is consistent with experimental observations by Leśniewska and Mróz (2001), as well as with FE analysis results by Gudehus and Nubel (2004). As shown in Fig. 2, the inclination angle of the shear bands in the retained soil mass with respect to the horizontal is larger in the case of dense than loose sand. A shear band running parallel to the wall back face also forms in all analyses, representing sliding between the sliding soil mass (wedge) and the wall.

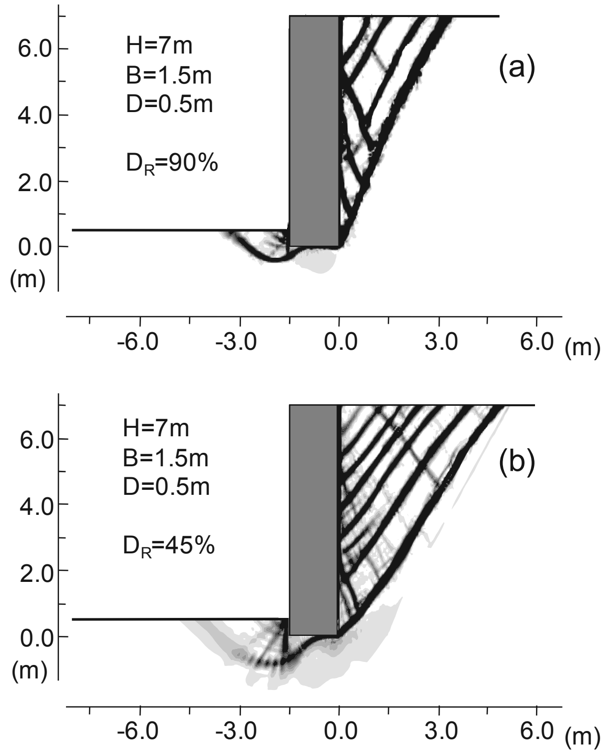

Figure 2. Contours of incremental γ_{max} from analyses with dense and loose Ottawa sand.

Below the wall base, a bearing capacity mechanism forms, the shape of which resembles that of mechanisms presented by Loukidis et al. (2008) for the case of strip footings on purely frictional material and subjected to eccentric and inclined loading.

3.2 *Active earth pressure evolution*

Fig. 3 illustrates how the normal (horizontal) stress distribution along the back of the wall changes during an analysis. At the beginning, there is the triangular stress distribution corresponding to geostatic stress conditions ($K=K_0$). With increasing wall displacement, the horizontal stress decreases progressively until a minimum active pressure state (MPS) is reached. From that point on, the average horizontal stress increases, but at a much lower rate than the rate at which it decreased earlier. Although before the MPS the stress distribution is smooth, afterwards, local peaks and valleys develop as consequence of bifurcation and the shear banding inside the sliding mass.

The evolution of the lateral earth pressure coefficient K with crest displacement u_C is shown in Fig. 4 for analyses with Toyoura sand with 60% relative density but different values of H, B, and D. It can be seen that K drops sharply towards a minimum value ($K_{A,min}$) corresponding to MPS at u_C approximately equal to $0.003H$ and, subsequently, rises smoothly, approaching a residual value ($K_{A,cr}$) related to the full development of critical state inside the sliding wedge. The results in Fig. 4 suggest that $K_{A,min}$ and $K_{A,cr}$ are practically independent of the wall dimensions and the embedment.

Fig. 5 shows the K/K_0 evolution for Toyoura and Ottawa sands with different values of relative density. The figure also shows the K_A value resulting from finite element analyses for an elastic-perfectly plastic soil following the Mohr-Coulomb failure criterion (M-C analyses) with friction angle ϕ equal to the critical state friction angle value ϕ_c of each sand for plane strain conditions and dilatancy angle ψ equal to zero (consistent with the constant volume response at critical state).

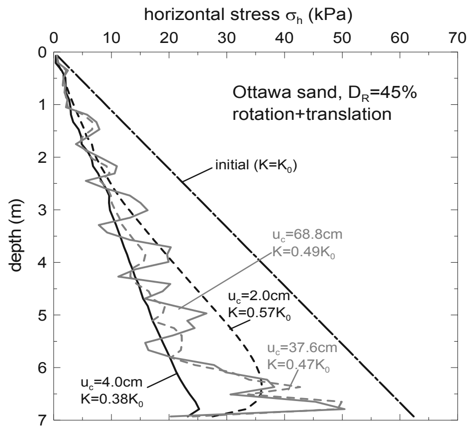

(a)

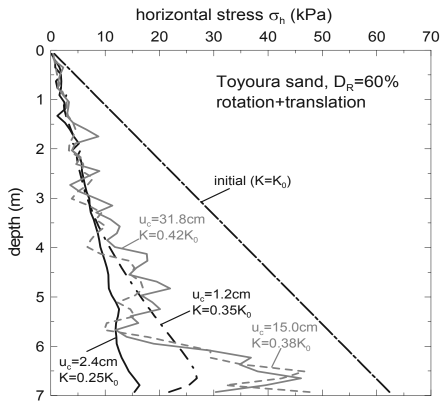

(b)

Figure 3. Examples of horizontal stress distribution acting on the wall backface at different stages during the analysis.

As expected, $K_{A,min}$ decreases with increasing relative density and, consequently, peak friction angle. The crest displacement required for reaching the MPS is in the $0.003H$ to $0.006H$ range, regardless the D_R value. On the other hand, attainment of $K_{A,cr}$ requires u_C larger than $0.10H$.

Interestingly, $K_{A,cr}$ seems also to depend on the relative density despite the fact that ϕ_c is independent of D_R. Only the curves for loose sand appear to attain $K_{A,cr}$ values that are in agreement with the K_A from the analyses with a perfectly plastic soil with material parameters consistent with critical state. This is because the inclination of the sliding plane delimiting the wedge depends on the dilatancy that the soil exhibits during the early stages of the wall movement, since the theoretical value of the shear band inclination with respect to the minor stress (i.e. horizontal) axis is equal to $45^o+(\phi+\psi)/4$ (Vardoulakis 1980). The sliding wedge forms at MPS, when the soil mass close to the wall is strongly dilative for all except very loose sand . Once the main inclined shear band forms, it tends to stay more or less at that location because of strain localization.

In most of the analyses, the u_C values required to cause bearing capacity failure of the wall foundation is in the $0.01H$ to $0.09H$ range, corresponding to toe displacement of $0.01B$ to $0.065B$. Hence, the foundation is expected to fail before full development of the residual active earth pressure state.

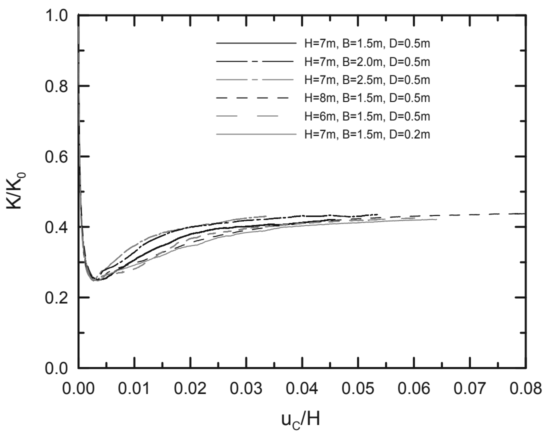

Figure 4. Variation of normalized lateral earth pressure coefficient with wall crest displacement from analyses with medium dense Toyoura sand (D_R=60%).

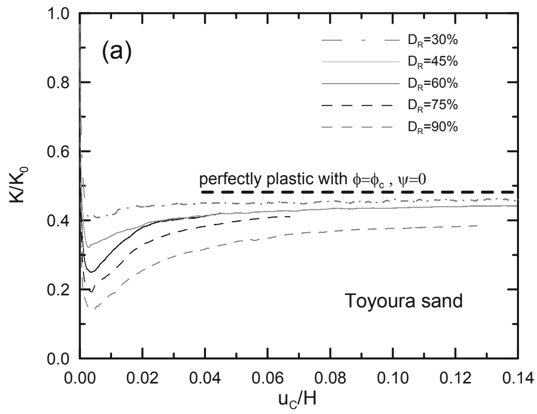

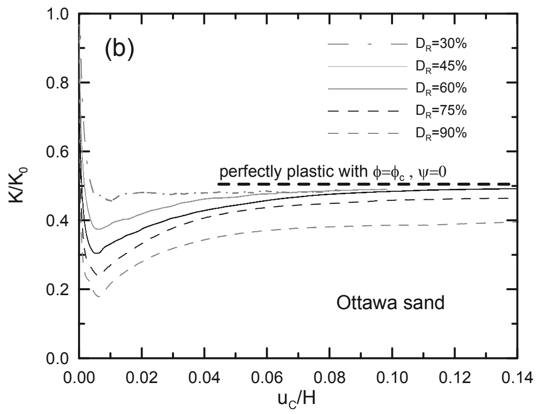

Figure 5. Variation of normalized lateral earth pressure coefficient with wall crest displacement from analyses of a wall with H=7m, B=1.5m and D=0.5m.

3.3 *Mobilized resistance along the wall-soil interface*

The mobilized friction coefficient μ (=tanδ) on the wall backface reaches a peak value at very early stages of the analyses, before the attainment of the MPS. After the peak, δ decreases quickly towards a residual value δ_c that is consistent with development of critical state inside the thin shear band that runs parallel to the wall backface. Despite this, it can be seen that the mobilized friction angle δ_{mob} at MPS ranges from 1.0 to 1.25 times the δ_c (Fig. 6). The δ_c values are 30.8^o and 29.6^o for Toyoura sand and Ottawa sand, respectively. These are consistent with the theoretical δ_c values calculated as arctan(sin$\phi_{c,PS}$), where $\phi_{c,PS}$ is the critical state friction angle for plane strain conditions. For Toyoura and Ottawa sands, this takes the values of 36.6^o and 34.6^o, respectively, which are roughly 4^o to 5^o larger than the values corresponding to triaxial compression conditions $\phi_{c,TX}$ (=31.6^o and 30.2^o, respectively).

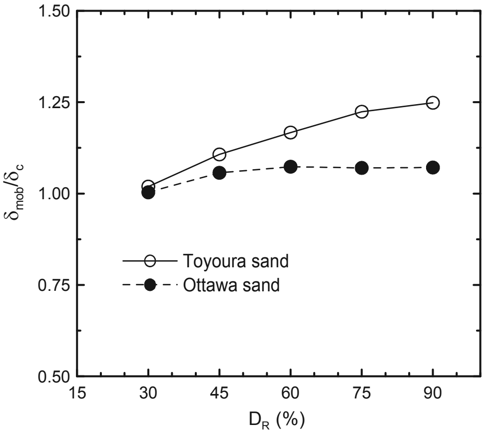

Figure 6. Ratio of the δ mobilized along the wall-soil interface at MPS to the δ corresponding to critical state conditions.

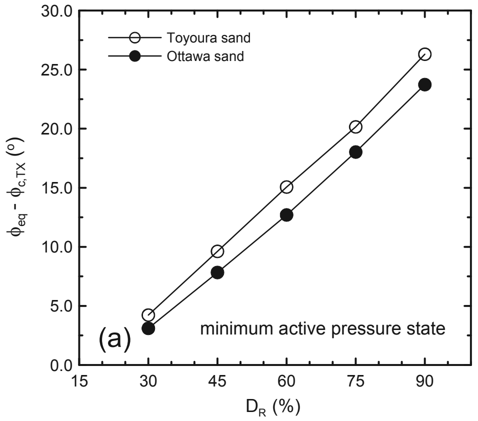

Figure 7. Equivalent value of the friction angle to be used in the calculation of $K_{A,min}$.

3.4 *Expression for the estimation of K_A*

The variation of the earth pressure coefficient K with crest displacement u_C observed in Figs. 4 and 5 can be described mathematically by the following equation:

$$K = \left[\frac{\dfrac{(K_0 - K_{A,cr})}{(K_0 - K_{A,min})} u_{Cp} - 2u_C}{\dfrac{u_{Cp}}{(K_0 - K_{A,min})} + \dfrac{u_C^{\,2}}{(K_{A,cr} - K_{A,min}) u_{Cp}}} \right] + K_{A,cr} \qquad (2)$$

where u_{Cp} is the crest displacement needed to reach MPS. Based on the previous discussion, u_{Cp} can be taken equal to $0.005H$.

The characteristic values of the active earth pressure coefficient, $K_{A,min}$ and $K_{A,cr}$, can be calculated using the Coulomb's equation (Eq. 1) with suitable (equivalent) values ϕ_{eq} for the mobilized friction angle inside the sliding wedge. In Fig. 7, we see that there is a linear dependence between ϕ_{eq} for MPS and $\phi_{c,TX}$, which can be expressed by

$$\phi_{eq}^{(MPS)} = \phi_{c,TX} + \left(35 \frac{D_R}{100\%} - 7^o \right) \qquad (3)$$

We consider $\phi_{c,TX}$ instead the more physically suitable $\phi_{c,PS}$ because it is easier to estimate through empirical relationships, measurements of the angle of repose on a conical soil heap, or a few triaxial compression tests. On the other hand, to calculate $K_{A,cr}$, the friction angle can be estimated using

$$\phi_{eq}^{(cr)} = \phi_{c,TX} + \left(9 \frac{D_R}{100\%} - 2^o \right) \qquad (4)$$

For the calculation of both $K_{A,min}$ and $K_{A,cr}$ using Eq. (1), the wall-soil interface friction angle δ can be conservatively set equal to δ_c estimated as arctan[sin($\phi_{c,TX}$+4^o)]. Finally, it should be pointed out that, according to the numerical results, the point of application of the active earth thrust at MPS is at a distance roughly $H/3$ from the wall base, while for the residual state is slightly smaller (roughly $0.3H$).

4 CONCLUSIONS

This paper presented the results of a set of finite element analyses of a retaining wall supporting sand. Based on numerical results, the active earth pressure coefficient attains a minimum value $K_{A,min}$ at wall crest displacements of the order of $0.005H$. Hence, from a practical standpoint, this state is of limited relevance to ultimate limit state (ULS) design; it is possibly representative of a serviceability limit state (SLS) design. A residual (maximum) value $K_{A,cr}$ associated to full mobilization of critical state inside the soil mass is practically reached at crest displacements of the order of $0.1H$.

The K_A to be used in ULS calculations can be estimated using the proposed Eq. (2), provided that the designer knows *a priori* the wall crest displacement u_C corresponding to ULS. In case there is a structure founded on the supported soil, the u_C can be set equal to the allowable foundation displacement value compatible with the ULS for the structure, established according to design code provisions. In the opposite case, the u_C could be set equal to 7 times the horizontal base displacmenet required for wall foundation failure. In the case of granular foundation soils, this base displacement can be conservatively taken as 0.05 times the base width.

5 REFERENCES

Abbo, A.J. and Sloan, S.W. 2000. *SNAC, User manual, Version 2.0*. Deptartment of Civil, Surveying and Environmental Engineering, University of Newcastle, Callaghan, Australia.

Dafalias, Y.F., Papadimitriou, A. G. and Li, X. S. 2004. Sand plasticity model accounting for inherent fabric anisotropy. *Journal of Engineering Mechanics*, ASCE, 130(11), 1319-1333.

Gudehus, G. and Nübel, K. 2004. Evolution of shear bands in sand. *Géotechnique*, 54(3), 187-201.

Lancellotta, R. 2002. Analytical solution of passive earth pressure. Géotechnique, 52(8), 617-619.

Leśniewska, D. & Mróz, Z. 2001. Study of evolution of shear band systems in sand retained by flexible wall. *International Journal for Numerical and Analytical Methods in Geomechanics*, 25, 909-932.

Loukidis, D. and Salgado, R. 2009. Modeling sand response using two-surface plasticity. *Computers and Geotechnics*, 36(1-2), 166-186.

Loukidis, D., Chakraborty, T. and Salgado, R. 2008. Bearing capacity of strip footings on purely frictional soil under eccentric and inclined loads. *Canadian Geotechnical Journal*, 45(6), 768-787.

Manzari, M.T. and Dafalias, Y.F. 1997. A critical state two-surface plasticity model for sands. *Géotechnique*, 47(2), 255-272.

Soubra, A-H and Macuh, B. 2002. Active and passive earth pressure coefficients by a kinematical approach. *Proceedings of the Institution of Civil Engineers – Geotechnical Engineering*, 155(2), 119-131.

Vardoulakis, I. 1980. Shear band inclination and shear modulus of sand in biaxial tests. *International Journal for Numerical and Analyrical Methods in Geomechanics*, 4(2), 103-119.